


 CrossMark
click for updates

 Cite this: *RSC Adv.*, 2014, 4, 57297

Sulfonated graphene as highly efficient and reusable acid carbocatalyst for the synthesis of ester plasticizers†

 Bhaskar Garg,^a Tanuja Bisht^b and Yong-Chien Ling^{*a}

Plasticizers are well known for their effectiveness in producing flexible plastics. The automotive, plastic and pharmaceutical industries, essential to a healthy economy, rely heavily on plasticizers to produce everything from construction materials to medical devices, cosmetics, children toys, food wraps, adhesives, paints, and 'wonder drugs'. Although H₂SO₄ is commonly used as commodity catalyst for plasticizer synthesis it is energy-inefficient, non-recyclable, and requires tedious separation from the homogeneous reaction mixture resulting in abundant non-recyclable acid waste. In this study, for the first time, we report an efficient synthesis of ester plasticizers (>90% yields) using sulfonated graphene (GSO₃H) as an energy-efficient, water tolerant, reusable and highly active solid acid carbocatalyst. The hydrothermal sulfonation of reduced graphene oxide with fuming H₂SO₄ at 120 °C for 3 days afforded GSO₃H with remarkable acid activity as demonstrated by ³¹P magic-angle spinning (MAS) NMR spectroscopy. The superior catalytic performance of GSO₃H over traditional homogeneous acids, Amberlyst™-15, and acidic ionic liquids has been attributed to the presence of highly acidic and stable sulfonic acid groups within the two dimensional graphene domain, which synergistically work for high mass transfer in the reaction. Furthermore, the preliminary experimental results indicate that GSO₃H is quite effective as a catalyst in the esterification of oleic and salicylic acid and thus may pave the way for its broad industrial applications in the near future.

 Received 25th September 2014
Accepted 23rd October 2014

DOI: 10.1039/c4ra11205a

www.rsc.org/advances

Introduction

Plasticizers or dispersants are one of the most critical accessory ingredients which play a vital role in the elaboration of plasticization efficiency and process performance¹ of a macromolecular material, especially, polyvinyl chloride (PVC),² one of the cheapest of all synthetic plastics currently used in daily life. Among plasticizers of industrial interest, esters of polycarboxylic acids such as citric acid have received significant attention owing to their low toxicity, compatibility with the host material, non-volatility as well as competitive price.³ Furthermore, the growing interest in biodegradable citric acid esters is mainly due to their ubiquity and importance in cosmetic, plastic, food, automobile, and pharmaceutical industries.⁴ Given the broad range of possible applications, it is predicted by the market research institute, Ceresana, that the worldwide

demand for plasticizers will increase to more than 7.6 million tonnes per year until 2018.⁵ The search for alternative approaches employing highly efficient and eco-friendly catalysts in the synthesis of plasticizers is, therefore, acute.

In industry, liquid-acid catalysts such as H₂SO₄ and methanesulfonic acid are predominantly used as crucial bulk commodity catalysts for the synthesis of ester plasticizers. However, these catalysts require challenging processes for their separation from the homogeneous reaction mixture, thereby resulting in abundant non-recyclable acid waste.⁶ To address these issues, endeavours have been made using alternative acid catalysts such as titanate,⁷ polyoxometalates (POMs),⁸ Zr-MCM-41,⁹ and acid functional ionic liquids (ILs)¹⁰ to complement liquid-acid catalysts in the synthesis of ester plasticizers. The as-mentioned catalysts certainly overcome some shortcomings but still are inappropriate due to the operational loss, high mass transfer resistance, deactivation, dissolution, and high cost. In this context, it is critical to search for a catalyst that combines the toxicological benefits of metal-free and cost-effective synthesis with the convenience of heterogeneous workup, whilst retaining the high activity in the synthesis of plasticizers.

Indubitably, the electronic "boom" that the world has experienced during the last decade is only due to one specific material, 'Graphene'. Graphene can be defined as a two dimensional sp² hybridized single-layer carbon sheet with

^aDepartment of Chemistry, National Tsing Hua University, 101, Section 2, Kuang-Fu Road, Hsinchu, 30013, Taiwan. E-mail: ycling@mx.nthu.edu.tw; Fax: +886 35727774; Tel: +886 35715131 ext. 33394

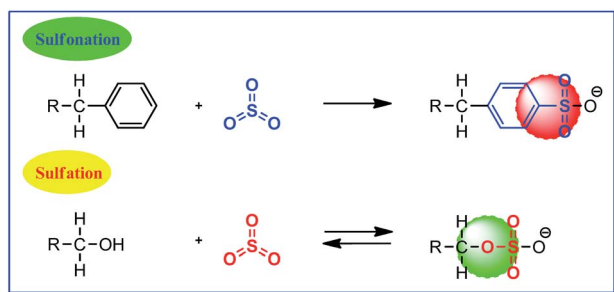
^bDepartment of Chemistry, Government Degree College, Champawat, 262523, Uttarakhand, India

† Electronic supplementary information (ESI) available: The characterization data and copies of selected ¹H and ¹³C NMR spectra of ester plasticizers. See DOI: 10.1039/c4ra11205a

hexagonal packed lattice (honeycomb) structure.¹¹ Owing to its exceptional properties,¹² graphene has been increasingly used for wide technological applications¹³ including photocatalysis.¹⁴ On another front, carbocatalysis by graphene is relatively new but rapidly emerging research area at the interface of organic, green, and material chemistry.¹⁵ The discovery that graphene oxide (GO) has an intrinsic acid activity¹⁶ has provided a handle for the development of graphene-based materials for a variety of acid catalysed reactions.¹⁷ Certainly, however, this growing interest in graphene-based acid catalysis has resulted 'an unsweet smell' of conceptual vagueness in many aspects.¹⁷ For instance, the surface modification of GO with sulfonated and sulfated groups is often confused while the structural differences between sulfonation and sulfation reactions are quite significant as shown in Scheme 1. Despite this, the fabrication of graphene with $-\text{SO}_3\text{H}$ groups affording sulfonated graphene is of crucial importance and increasingly used in catalysis,^{18a} micro-solid-phase extraction,^{18b} graphene-based composites,^{18c} biomimetics,^{18d} and other technological applications.^{18e-g}

Among different strategies for grafting $-\text{SO}_3\text{H}$ groups in graphene domain, oleum-assisted sulfonation has appeared as an attractive strategy.¹⁹ Nevertheless, alternative reaction conditions, an upscale synthesis at relatively low cost, and the simplicity in processing and handling are some of the important tenets of 'green chemistry' and can be the best selections in the catalysis research. Equally important is to investigate and expanding the scope of existing catalysts for possible industrial applications. With these realizations combined with a knowledge of products-switching in tetrapyrrolic systems using acidic ionic liquid catalysts,²⁰ we decided to investigate an energy-efficient, upscale, and alternative synthesis methodology for oleum-assisted sulfonation of graphene and expanding the scope of as-prepared sulfonated graphene (GSO_3H) to novel applications such as in the synthesis of (biodegradable)ester plasticizers. To the best of our knowledge, there is still no report of using graphene-based solid acid catalysts in the aforementioned synthesis.

Intrigued by the significant role of polycarboxylic acid esters in automotive, food, plastic and polymer industries combined with our ongoing interest in homo- and heterogeneous catalysis,^{21,22} herein, we report the synthesis of highly active GSO_3H , a solid acid catalyst and its usefulness in the effective synthesis of ester plasticizers. In line with this, the scope of GSO_3H is



Scheme 1 Sulfonation vs. Sulfation reactions. Reproduced from ref. 17.

further extended and examined in the esterification reactions of oleic and salicylic acid.

Results and discussion

Preparation and characterization of GSO_3H

Considering the practical applications of GSO_3H , the bulk synthesis of GO was the prerequisite in this study. However, it is well known that during washing/purification steps, GO dispersions tend to undergo severe gelation rendering filtration more complicated and tedious.²² Taking this into account, an acid-acetone washing procedure was adopted for preventing gelation and speeding-up the purification step in the synthesis of GO.²³ Furthermore, it is also identified that LiAlH_4 is one of the strongest reducing agents in hydride family and serves as an attractive option, where most reducing agents exhibit moderate reactivity toward carboxyl functions. Accordingly, LiAlH_4 was applied for reduction of GO into reduced graphene oxide (rGO).

Fuming H_2SO_4 or oleum-assisted sulfonation is one of the simple and efficient industrial strategies, especially, for versatility in feedstock selection to build materials that are truly application specific. Nevertheless, relatively high temperature conditions used in sulfonation reaction of rGO may introduce some defects within graphene domain resulting in an insufficient grafting of $-\text{SO}_3\text{H}$ groups, which, in turn, will lower the acid density of sulfonated material resulting in limited catalysis. Consequently, the oleum-assisted sulfonation of rGO was performed at relatively low temperature for several days. The present protocol not only avoids the use of expensive instrument handling but also permits the bulk synthesis of GSO_3H with ease.

The Fourier transform infrared spectroscopy (FT-IR) spectrum of GO as shown in Fig. 1 presented substantial bands at 1054 and 1400 cm^{-1} corresponding to C-OH vibrations. The signal at 1230 cm^{-1} was generated by stretching vibrations of C-O-C groups, and finally, two intense bands at 1623 and 1729 cm^{-1} were generated by C=O and -COOH vibrations, respectively.²⁴ Compared with GO, GSO_3H exhibited one prominent

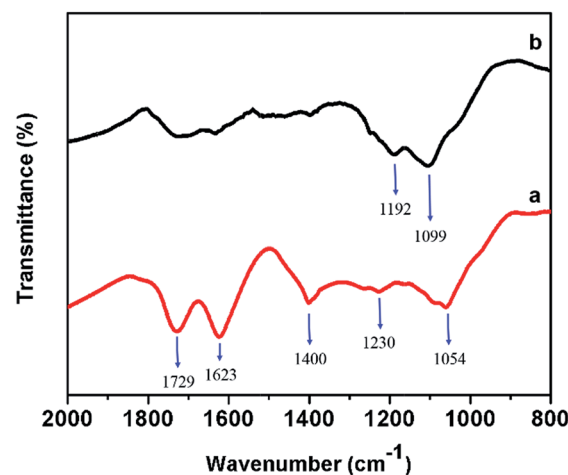


Fig. 1 FT-IR spectra of (a) GO and (b) GSO_3H .

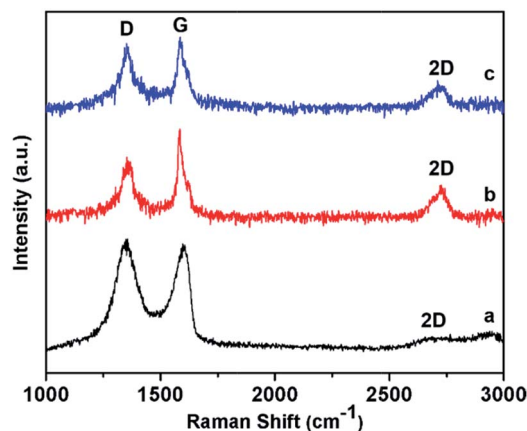


Fig. 2 Raman spectra of (a) GO, (b) rGO, and (c) GSO₃H.

band at 1099 cm⁻¹ and relatively a weak band at 1192 cm⁻¹, which are associated with S=O stretching vibrations.^{19,25} However, similar to that of rGO (not shown here), the bands at 1729, 1623, 1400, 1054 and 1230 cm⁻¹ were severely attenuated in the spectrum of GSO₃H. These results combined with the ³¹P magic-angle spinning (MAS) NMR spectroscopy, as will be discussed below, confirmed the successful grafting of -SO₃H groups in the as-prepared GSO₃H.

In order to gain the structural information about GO, rGO and GSO₃H, Raman spectroscopy was used. As shown in Fig. 2, the first-order Raman spectra of GO exhibited two characteristic D (indicative of the defects and ordered/disordered structure of graphitic carbon) and G bands (indicative of pristine graphene sheet) at 1354 and 1599 cm⁻¹, respectively. The obtained I_D/I_G ratio of GO was 1.04 indicating an extensive disorder in the graphitic structure due to the presence of a complex cocktail of oxygen functionalities. Upon reduction, the rGO exhibited quite similar Raman spectra to that of GO, however, the I_D/I_G ratio decreased to 0.85. A reduced I_D/I_G ratio can be attributed to the removal of oxygen-containing groups and the reintroduction of large aromatic domains.²⁶ Compared with rGO, GSO₃H gave relatively a higher I_D/I_G ratio (0.98) suggesting a decrease in the

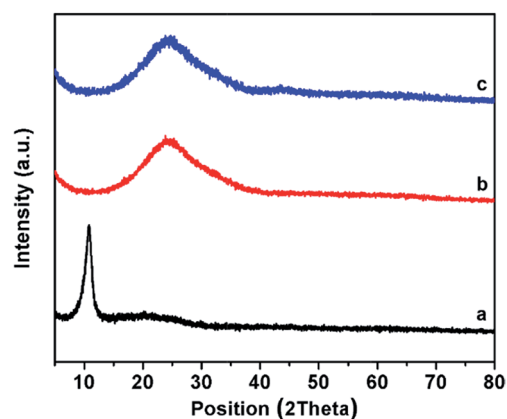


Fig. 3 XRD patterns of (a) GO, (b) rGO, and (c) GSO₃H.

average size of sp² hybridized graphene domains due to the incorporation of abundant -SO₃H groups.²⁵

Fig. 3 shows the X-ray diffraction (XRD) patterns of GO, rGO, and GSO₃H. GO displayed a sharp peak at 10.7° at the expense of a diffraction peak at 26.2°, associated with graphite. The appearance of a peak at 10.7° clearly indicates the presence of oxygen functionalities in graphene domains. Upon reduction, the peak at 10.7° completely disappeared and rGO exhibited a broad diffraction peak, centred at 24.2°. The GSO₃H showed almost similar XRD patterns (24.2°)¹⁹ as rGO which suggests their similar graphene domains.

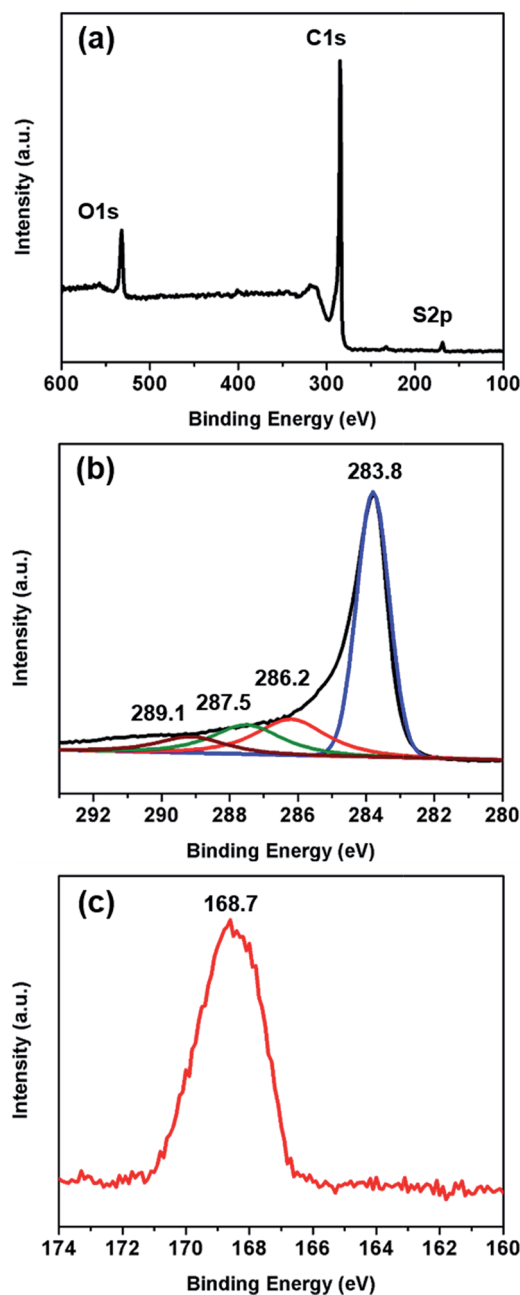


Fig. 4 XPS spectra of the GSO₃H; (a) Survey spectrum. (b) High resolution C1s. (c) S2p spectrum.

To investigate the surface composition and chemical state of the elements, GSO₃H was further characterized by X-ray photoelectron spectroscopy (XPS) analysis. As shown in Fig. 4a, the XPS spectrum of as-prepared GSO₃H displayed a predominant C1s peak, a weaker O1s and much weaker S2p peak. In detail, the high resolution C1s XPS spectrum (Fig. 4b) can be deconvoluted into four peaks at 283.8, 286.2, 287.5 and 289.1 eV which are respectively attributed to C–C, C–O–C, C=O, and O=C–OH species.¹⁹ Notably, the intensities for the peaks corresponding to the carbonyl and the carboxylate functions exhibited much smaller relative contents suggesting that most of the oxygen-containing functional groups are successfully removed in GSO₃H.²⁷ The S2p spectrum of GSO₃H showed a peak at 168.7 eV (Fig. 1c), which is slightly lower than those of –SO₃H functionalized ordered mesoporous carbon (OMC–SO₃H; 168.8 eV), Amberlyst™-15 (168.9 eV), and sulfonated hollow sphere carbon (HSC–SO₃H, 169.1 eV).^{19,28} In this milieu, it is important to stress that binding energy of S2p is a direct measure and quite sensitive to the acidic strength.²⁹

The elemental analysis was performed with GO, rGO and GSO₃H. Specifically, GO and rGO resulted in C/O ratios of 1.09 (C, 49.01%; O, 44.56%) and 13.5 (C, 89.2%; O, 6.6%), respectively. An increase in the C/O ratio in rGO certainly signify the efficacy of LiAlH₄. Alongside, the elemental analysis revealed that the mass ratios of carbon, oxygen and sulphur in GSO₃H are 86.48, 8.56, and 4.96%, respectively. That is, the density of –SO₃H groups in GSO₃H is calculated to be 1.55 mmol g⁻¹. However, the acid–base titrations revealed that GSO₃H has an actual acid exchange capacity of 1.69 mmol H⁺ g⁻¹. This is,

presumably, due to the presence of O-acid sites, in particular, hydroxyl functions, other than –SO₃H group on the surface of GSO₃H. Considering the higher O/S atom ratio (3.4 : 1) than the theoretical one (3 : 1), the presence of residual oxygen-containing functional groups on GSO₃H surface is further confirmed. Aside from the GSO₃H, the neutralization titrations of GO indicated an acid exchange capacity of 0.89 mmol H⁺ g⁻¹, which may be attributed to the presence of –O–SO₃H groups on the surface of GO.

In order to further shed light on the acid strength of as-prepared GSO₃H, ³¹P MAS NMR spectroscopy was executed using triethylphosphine oxide (TEPO) as an adsorbed base probe molecule. Indeed, this method has been shown to be sensitive and reliable technique capable of providing exclusive information about relative acidities of various solid acids. In particular, the larger ³¹P NMR chemical shifts ($\delta^{31}\text{P}$) correlates the higher acidic strength of respective solid acid.³⁰ Fig. 5 shows the ³¹P NMR spectrum of TEPO adsorbed on different extracted materials: GO, rGO, GSO₃H, and a sulfonic resin, Amberlyst™-15.

Spectrum for rGO (as prepared by LiAlH₄ triggered reduction of GO) exhibited a broad ³¹P peak centred at 55.5 ppm that may correspond to TEPO adsorbed on residual –OH and –COOH groups on the surface of rGO. The as-prepared GSO₃H shared a resonance at nearly same chemical shift (58.3 ppm) as rGO and is in accordance with results reported by other authors.³¹ However, relatively a high intensity of this peak than that of rGO may be attributed to the introduction of additional oxygen-containing groups during sulfonation reaction of rGO. In addition, GSO₃H exhibited two overlapping but strong ³¹P NMR

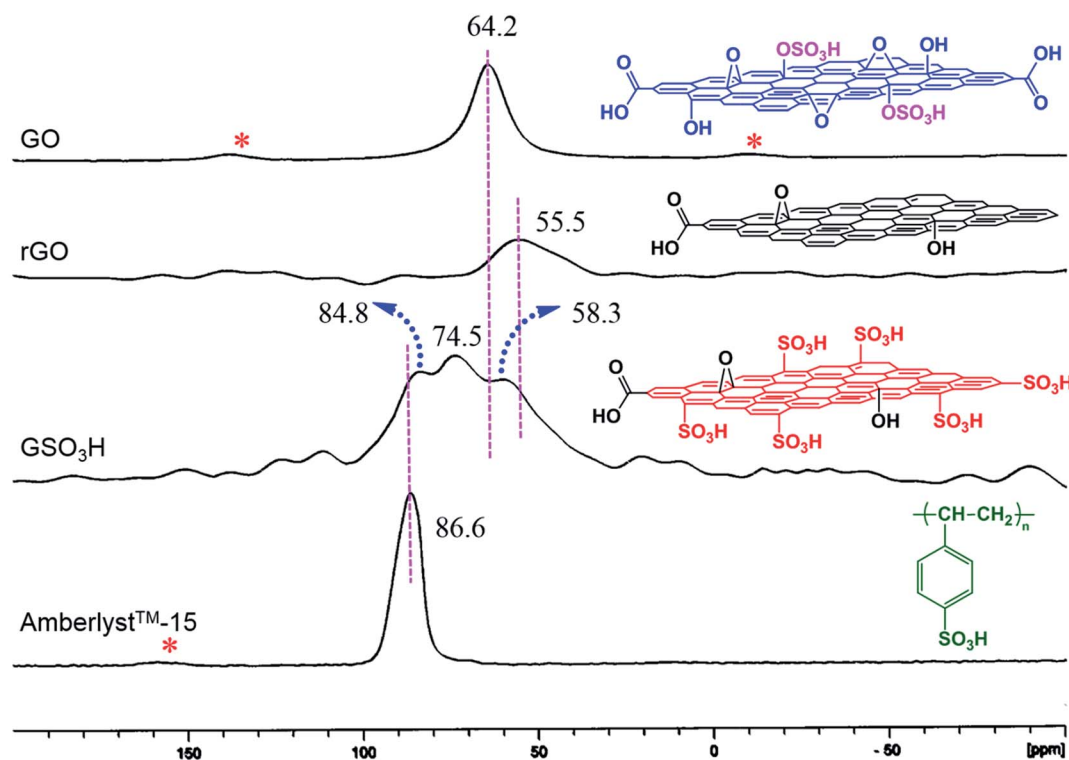


Fig. 5 ³¹P NMR spectra of TEPO chemically adsorbed onto GO, rGO, GSO₃H, and Amberlyst™-15. The asterisks mark spinning sidebands.

signals at 74.5 and 84.8 ppm, respectively, authenticating the presence of highly acidic $-\text{SO}_3\text{H}$ groups on the surface of graphene domains. Interestingly, the signal at 84.8 ppm is in good agreement with AmberlystTM-15, which displays a very high acidity (86.6 ppm;³² single, sharp and strong resonance) due to the presence of a macro reticular sulfonic polystyrene network. These results clearly demonstrate that just by simple switching in experimental conditions, highly acidic sulfonated graphene can be obtained with ease.

Aside from these observations, the ^{31}P NMR spectrum of GO displayed a single strong resonance at 64.2 ppm that may be connected to the TEPO adsorbed on mixed acidic centers arising from the presence of hydrosulphates ($-\text{O}-\text{SO}_3\text{H}$) in conjunction with abundant $-\text{OH}$ groups. It would be worthwhile to mention here that the acidic strength of GO is nearly comparable to aluminium-substituted mesoporous silica (Al-MCM-41; 66–69 ppm) or even significantly higher than that of conventional SBA-15 mesoporous silica (~ 60 ppm) as evaluated by TEPO adsorbed ^{31}P NMR chemical shifts.³²

Fig. 6 depicts the field-emission scanning electron microscopy (FESEM) images of GO, rGO, and GSO_3H . The FESEM image clearly indicates the layered structure of GO (Fig. 6a). Compared with GO, the rGO (Fig. 6b) exhibited crumpling features in exfoliated graphene domains. The sulfonation of rGO led to further exfoliation (Fig. 6c) of crumpled layers into sheet-like structure as evidenced by high resolution FESEM image (Fig. 6d). Indeed, to some extent, the crumpling features

can also be seen in GSO_3H that may have the potential advantage in heterogeneous acid catalysis.

Catalytic activity of GSO_3H : optimization of the reaction conditions

Having established the essential nature of the GSO_3H , the conversion of citric acid (**1**) and *n*-butanol (**2a**) into tributyl citrate (**3a**) was chosen as a model reaction in order to explore the catalytic activity of GSO_3H under different reaction conditions. (Table 1). In a preliminary experiment, **1** (5.2 mmol) in **2a** (25 mL) was refluxed for 4 h in the presence of GSO_3H (200 mg). To our delight, after filtration of catalyst and removal of the volatile solvent, **3a** could be obtained in an excellent yield of ca. 94% (Table 1, entry 3).

After observing quantitative conversion of **1** into **3a**, subsequent efforts were directed toward optimizing reaction conditions such as GSO_3H loadings and the reaction time. In particular, minimal changes in the isolated yields were observed upon increasing the reaction time and GSO_3H loadings (Table 1, entries 4–6). Nevertheless, it was found that variations in the GSO_3H loadings (ranging from 50–100 mg) had a significant effect on the isolated yields of the plasticizer products (Table 1, entries 1, 2). While 50 mg of GSO_3H afforded 35% of the target product (Table 1, entry 1), increasing the loading to 200 mg of GSO_3H was found to be sufficient to drive the esterification reaction in the forward direction (Table 1, entry 3). When **2a** was employed in stoichiometric amount (3.2

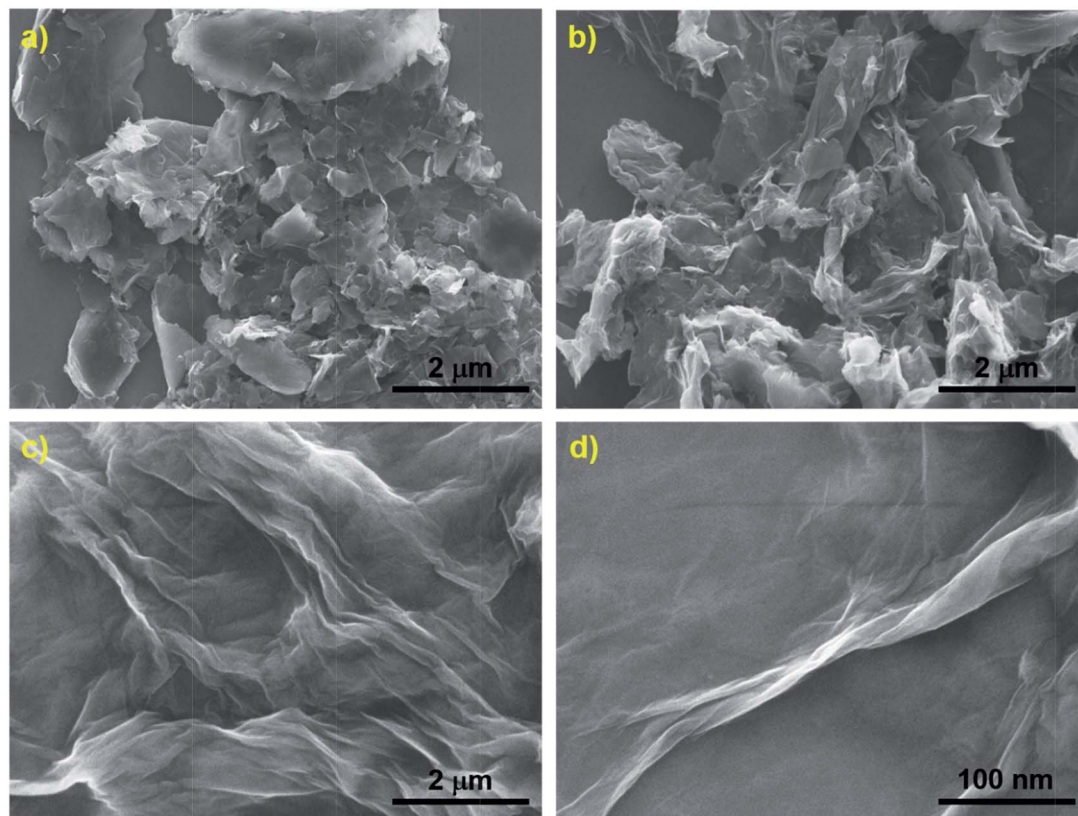
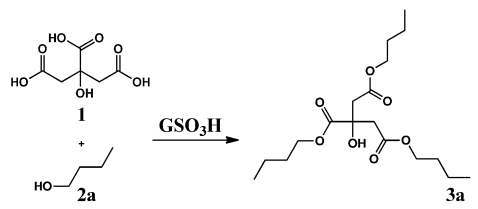


Fig. 6 The FESEM images of (a) GO, (b) rGO, and (c and d) GSO_3H .

Table 1 Esterification of citric acid (**1**) with *n*-butanol (**2a**) into tributyl citrate (**3a**) over GSO₃H and other catalysts^a



Entry	Catalyst	Loading	Time (h)	Yield ^b (%)
1	GSO ₃ H	50 mg	4	35
2	GSO ₃ H	100 mg	4	69
3	GSO ₃ H	200 mg	4	94
4	GSO ₃ H	200 mg	6, 8	92, 90
5	GSO ₃ H	300 mg	4	93
6	GSO ₃ H	400 mg	4	93
7 ^c	GSO ₃ H	200 mg	4	90
8	—	—	4, 8, 10, 12	—
9 ^d	GSO ₃ H	200 mg	4	56 ^e , 64 ^f , 92 ^g
10	GO	200 mg	4	42
		400 mg		62
11	r-GO	200 mg	6–8	5
12	Graphite	200 mg	6–24	2.3
13	H ₂ SO ₄	3 mol%	4	94
14 ^h	<i>p</i> -TSA	5 mol%	4	78
15 ⁱ	H ₃ PW ₁₂ O ₄₀	5 mol%	4	70
16 ^j	Amberlyst™-15	10 wt%	4	79
17 ^k		6 mL	4	94
18 ^l		5 mL	4	Dissolved
19 ^m		5 mL	4	Dissolved

^a Reaction conditions: **1** (5.2 mmol), **2a** (25 mL), and catalyst (type and amount indicated) were combined in 50 mL round-bottomed flask and refluxed at 120 °C unless otherwise stated for the time indicated.
^b Isolated yield. ^c After five runs. ^d **1** (5.2 mmol), **2a** (16.6 mmol), and solvent (25 mL). ^e DCM, 45 °C. ^f THF, 75 °C. ^g Toluene, 112 °C.
^h *p*-Toluene sulfonic acid. ⁱ Phosphotungstic acid. ^j Catalyst was activated at 105 °C for 4 h and dried prior to use. ^k Dried under vacuum for 6 h and stored in dry box prior to use; **1** (5.2 mmol).
^l Dried under vacuum for 6 h and stored in dry box prior to use; **2a** (16.6 mmol). ^m Dried under vacuum for 6 h and stored in dry box prior to use; 90 °C.

equiv.) in the presence of different solvents, **3a** was obtained in moderate to excellent yields (Table 1, entry 9). The relatively lower yield of **3a** in DCM and THF may be attributed to the effect of refluxing temperature and consequently lower reaction rate. Importantly, the conversion of **1** into **3a** was quantitative in toluene (Table 1, entry 9).

To verify whether or not the catalysis is truly heterogeneous or due to some leached active species present in the liquid phase, the reaction was carried out under the optimized conditions as described in Table 1 and the GSO₃H was filtered

from the reaction mixture at *ca.* 50% formation of **3a**. After removal of the GSO₃H, the reaction was progressed again at reflux. In the absence of GSO₃H, no further product formation was observed even after 2 h indicating that catalysis occurs on the surface of GSO₃H and the process is truly heterogeneous. These experiments clearly demonstrate the indispensable role of GSO₃H in facilitating the esterification reaction to quantitative conversion.

In the reaction of **1** with **2a**, GO exhibited good catalytic activity (though poorer than GSO₃H), when used at higher doses under otherwise optimized conditions (Table 1, entry 10). The catalytic activity of GO might be attributed to its inherent acidic nature due to the presence of surface functional –O–SO₃H groups, which can be introduced during the synthesis of GO under relatively harsh acidic conditions.³³ Nevertheless, minimal yields of the plasticizer product were obtained when GSO₃H was replaced by natural flake graphite or rGO (Table 1, entries 11, 12). Likewise, no product formation was recognized in the absence of a carbon promoter under otherwise identical conditions (reflux, 4 h) or even prolonging the reaction time (Table 1, entry 8).

Comparison of GSO₃H activity with other acid catalysts

To evaluate the catalytic performance of GSO₃H, various traditional acid catalysts were also examined and the results are summarized in Table 1. Specifically, homogeneous acids such as H₃PW₁₂O₄₀, *p*-toluenesulfonic acid (*p*-TSA), and H₂SO₄ were examined in the reaction and afforded **3a** in good (70%, 78%) to excellent (94%) yields, respectively (Table 1, entries 13–15).

A relatively high yield of **3a** in the presence of H₂SO₄, comparable to that use of GSO₃H, was not surprising as H₂SO₄ exhibits higher acidity than those of H₃PW₁₂O₄₀ and *p*-TSA. Furthermore, the unique spatial separation as well as the self-similarity of structures between the active sites in H₂SO₄ allow consistent energetic interactions between each of active site and reaction substrate. However, the technical challenges, of either the separation issue associated with H₃PW₁₂O₄₀ or reuse performances of these homogeneous acids were of high concern.

Aside from homogeneous acids, Amberlyst™-15 was of further interest due to its established activity in important acid-catalyzed reactions such as esterification, and alkylation.³⁴ The reaction of **1** with **2a** in the presence of Amberlyst™-15 afforded **3a** in 79% yield (Table 1, entry 16). Considering the much higher acidic content of Amberlyst™-15 (4.7 eq. per kg)³⁴ than that of GSO₃H, the higher catalytic activity of GSO₃H over Amberlyst™-15 may be associated to its unique two dimensional sheet structure, where most of the –SO₃H groups are well dispersed and exposed to the reactants resulting in the high mass transfer. The another possible explanation for the stronger acidity of the GSO₃H is that some of the –SO₃H groups in GSO₃H may be linked by strong hydrogen bonds ensuing in the higher acidity due to mutual electron-withdrawal.³⁵ On the other hand, Amberlyst™-15 represents a porous structure resulting in relatively slow mass transfer. As a consequence, some of the –SO₃H

groups on this porous catalyst might not be accessible to reactants and thus limit the product yield to a reasonable extent.

Indubitably, ILs have been under the spotlight of the green catalysis over the last decade.³⁶ Consequently, the final catalysts screened were of acid functionalized Brønsted ILs which were of particular interest to us after observing their unique catalytic potential in the organic synthesis^{20,21b} as well as in the rapid identification of tertiaryalkyl amines.³⁷ Stirring **1** with **2a** in the presence of *N*-(4-sulfonic acid) butyl triethylammonium hydrogen sulfate [TEBSA][H₂SO₄] at 90 °C for 4 h afforded a clear biphasic reaction mixture. The upper phase was simply decanted and the desired **3a** could be obtained in 94% yield (Table 1, entry 17). The obtained yield was comparable to that of H₂SO₄ and GSO₃H. Nevertheless, during the reaction, both *N*-methyl-2-pyrrolidonium hydrogen sulfate [NMP][H₂SO₄] and *N*-methyl-2-pyrrolidonium methane sulfonate [NMP][CH₃SO₃] dissolved in the reaction mixture making it difficult in separation (Table 1, entries 18, 19).

Reusability of GSO₃H

The reusability of GSO₃H in conjunction with [TEBSA][H₂SO₄], and Amberlyst™-15 was investigated for the esterification reaction of **1** with **2a** under identical conditions as described in Table 1 and Fig. 7. In general, after the reaction, the catalysts were separated from the reaction mixture and reused without any further treatment except vacuum drying. Interestingly, the yield was significantly reduced in the next cycle (<50%) when Amberlyst™-15 was used. This may be attributed to that of the water-induced poisoning of the porous acidic sites in Amberlyst™-15. On the other hand, [TEBSA][H₂SO₄] was dissolved in the reaction mixture after three consecutive cycles.

GSO₃H exhibited remarkable activity and could be reused between the first and fifth runs without any considerable loss in the catalytic activity (Table 1, entry 7). It should be noted that unlike –SO₃H bearing resins, the reaction with the carbocatalyst is not significantly dependent on the amount of water present in the reaction system³⁸ resulting in the high activity of GSO₃H in esterification reactions. In addition, because GSO₃H possess –SO₃H and few –COOH functions, it is expected that electron-withdrawing nature of –COOH can increase the electron density between the carbon and sulphur atoms resulting in the

greater stability of the GSO₃H even under harsh reaction conditions.

Catalytic scope of GSO₃H

The scope and limitations of GSO₃H were examined by screening a variety of structurally diverse alcohols **2b–2h** in the synthesis of biodegradable ester plasticizers such as trimethyl citrate (TMC), triethyl citrate (TEC), triisopropyl citrate (TIPC), triisobutyl citrate (TIBC), tri-*n*-hexyl citrate (THC), tri-*n*-active amyl citrate (TAAC), and tri-*n*-octyl citrate (TOC).

As revealed in Table 2, the reaction of **1** with **2b–2h**, regardless of the presence of linear (Table 2, entries 1–4) or branched chain (Table 2, entries 5–7) functionalities could be directly converted to their respective plasticizer products in appreciable yields. Despite being all primary alcohols, the reactivity of alcohols having long alkyl chain appeared slightly lower (Table 2, entries 3, 4) than that of short or branched chain alcohols (Table 2, entries 1, 2 and 5–7). Furthermore, **2g** exhibited the shortest reaction time, presumably, because of its stronger nucleophilic activity over primary alcohols. Nevertheless, the formation of mono- and di-esterification products was not recognized in any case under the experimental conditions.

In an effort to expand GSO₃H activity within the family of ester plasticizers, we turned next toward exploring the synthesis of phthalic acid esters. The so called ‘phthalate plasticizers’ found applications for the first time in 1920s and by far are the most widely used plasticizers, primarily, to make soft and flexible PVC, in the 21st century.³⁹ With phthalates, the polarisable benzene nucleus is highly effective with respect to compatibility with PVC, making the long polyvinyl molecules to slide against one another. Considering the greater return upon charging and less water to expel (in comparison to traditional acid catalysts) at the end of esterification reaction, phthalic anhydride **4** is used as a precursor rather than phthalic acid. As summarized in Table 3, a broad range of alcohols **2** were successfully converted to their corresponding plasticizers using GSO₃H under optimized conditions (7.0 mmol **4**, 150 mg GSO₃H, 20 mL solvent, and reflux). Excellent yields (>92%) of plasticizers were obtained in all the cases including those that featured long or branched O-alkyl substituents.

Considering its significant biodegradability, lower carbon dioxide/sulphur emission, and minor particulate pollutants, biodiesel consisting of long-chain fatty acid alkyl esters (FAAE) can be used both as an alternative fuel and as an additive for petroleum diesel. On another front, methyl salicylate (MS) or oil of wintergreen is an industrially important fine chemical. Intrigued by the successful use of solid acid catalysts in the production of biodiesel by esterification,⁴⁰ a further attempt was made to extend the feasibility of GSO₃H in the esterification of oleic acid to methyl oleate (MO) as well as in the synthesis of MS.

As depicted in Table 4, the GSO₃H catalysed esterification of oleic and salicylic acid gave excellent conversions within 4 h. Furthermore, the catalyst was equally effective during second run demonstrating the superior catalytic performance of GSO₃H. The effect of variable reaction conditions on product

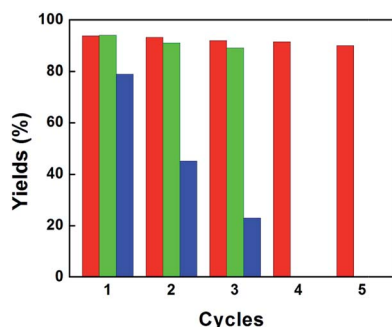
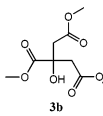
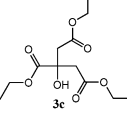
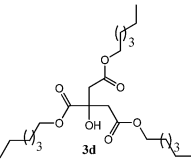
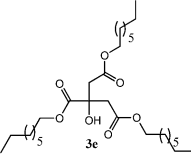
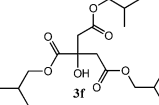
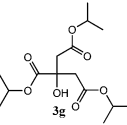
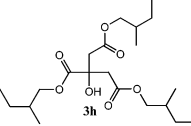


Fig. 7 The recycle activity of GSO₃H. Bars denote as: blue bar (Amberlyst™-15), green bar ([TEBSA][H₂SO₄]), and red bar (GSO₃H).

Table 2 Synthesis of biodegradable plasticizers using GSO₃H^a

Entry	Alcohol (2)	Molar ratio of 1 : 2	Product (3)	Method	Time (h)	Yield ^b (%)
1 ^c		1 : excess		Method A	4	93
2 ^c		1 : excess		Method A	4	94
3		1 : 3.2		Method B ^d	6 ^e	88
4		1 : 3.2		Method B ^d	6 ^e	87
5		1 : 3.2		Method B ^d	4	91
6		1 : excess		Method A	2.5	94
7		1 : 3.2		Method B ^d	4 ^e	93

^a All reactions were performed at 90 °C without solvent using 5.2 mmol citric acid 1, 200 mg GSO₃H for the indicated reaction time. GSO₃H was kept under high vacuum for 3 h prior to use. ^b Isolated yield. ^c HPLC grade solvents were used. The solvents were further dried and distilled by following the standard procedures prior to their use. ^d Toluene was the solvent of choice, 25 mL, 112 °C. ^e After 4 h, the progress of the reactions were scrutinized in every 30 min by TLC. After filtration of catalyst and subsequent removal of solvent, the product was passed through a short silica column and dried.

formation, however, must await a more detailed systematic study in this regard.

Experimental

Chemicals and reagents

Natural graphite flake (7–10 micron, 99%), 1-hexanol, 1-butanol, triethylamine, 1,4-butane sultone, phthalic anhydride were purchased from Alfa Aesar, UK. *N*-methyl-2-pyrrolidone, 2-methyl-1-propanol, 2-methyl-1-butanol, Amberlyst™-15, *p*-TSA, glycerol, NaNO₃, H₂SO₄, and Oleum (30% SO₃) were purchased from Sigma-Aldrich. Anhydrous citric acid, methanol, 1-octanol, 2-propanol, THF, and DCM were purchased from J. T. Baker (USA). Lithium aluminium hydride

(LAH) was purchased from Lancaster. KMnO₄ was obtained from Fluka. Toluene (100% assays by GC) was purchased from Mallinckrodt chemicals. All chemicals and reagents received were of highest purity and used without further purification unless otherwise mentioned.

Methods

Fisher Scientific FS60 ultrasonic bath cleaner (150 W) was used for performing sonication treatment of G-NMs. The XRD patterns were recorded using a Shimadzu XRD-600 diffractometer with CuK α radiation. The morphology of G-NMs were examined using FESEM (Hitachi, S-4800, 15 kV). The XPS measurements were carried out using an ULVAC-PHI Quantera

Table 3 Synthesis of phthalate plasticizers using GSO₃H^a

Entry	Alcohol (2)	Molar ratio (4 : 2)	Product (5)	Method	Time (h)	Yield ^b (%)
1		1 : excess		Method A	4	94
2		1 : excess		Method A	3	96
3		1 : excess		Method A	3	93
4		1 : 2.1		Method B	6	92
5		1 : 2.1		Method B	6	95
6		1 : 2.1		Method B	4	95
7		1 : 2.1		Method B	4	96
8		1 : 2.1		Method B	5	94

^a All reactions were performed at reflux with (20 mL) or without solvent using 7.0 mmol phthalic anhydride **4**, and 150 mg GSO₃H for the indicated reaction time. The other reaction conditions are virtually the same as described above in Table 2. ^b Isolated yield.

Table 4 Esterification of oleic and salicylic acid with CH₃OH in the presence of GSO₃H^a

Entry	Conversion ^b (%)		Selectivity ^c (%)
	MO	MS	
1	98.9	95.7	100
2 ^d	98.6	95.6	100

^a Reaction conditions: ratio of CH₃OH to oleic acid and salicylic acid = 5 : 1; GSO₃H = 200 mg; refluxed for 4 h at 90 °C. ^b Based on GC analysis. ^c Selectivity for methyl salicylate (based on salicylic acid). ^d Reuse performance of GSO₃H.

SXM spectrometer and data were recorded using a monochromatic Al anode as the excitation source. The FT-IR was carried out on a Perkin-Elmer system 2000 (Perkin-Elmer,

Fremont, CA, USA). The confocal micro Raman spectroscopy was performed using a Horiba Jobin-Yvon LAB RAM HR 800 UV (Japan) spectrometer (laser source: 325 nm, He-Cd, 30 mW).

The ion-exchange capacities of the G-NMs were determined by acid–base titrations. In a typical experiment, 0.05 g of solid sample was added to aqueous solution of NaCl (0.1 M, 20 mL) and the resulting suspension was allowed to equilibrate. Thereafter, it was titrated by dropwise addition of aqueous NaOH (0.01 M).

The acid properties of solid G-NMs and Amberlyst™-15 were assessed by monitoring the ³¹P NMR chemical shift of chemically adsorbed TEPO onto the solid materials. In a typical experiment, TEPO (0.015 g) was dissolved in anhydrous pentane (5 mL), and this solution was mixed with dehydrated solid acids (0.15 g). The resulting suspension was allowed to equilibrate

under stirring for 30 min in an inert atmosphere and thereafter dried at 50 °C under vacuum.

The ^{31}P NMR measurements were performed on a Bruker Avance III 400 spectrometer using a 4 mm double resonance probe operating at a B_0 field of 9.4 T (400 MHz) with a ^{31}P Larmor frequency of 161.9 MHz. ^{31}P { ^1H } MAS NMR spectra were recorded by using a rotation speed of 12 kHz, a single excitation pulse width of 1.9 ms, a radio-frequency field strength of 45 kHz, and 15 s recycle delay. A two-pulse phase modulation scheme (TPPM-15) was used for ^1H heteronuclear decoupling.

The ^1H NMR and ^{13}C NMR were recorded on a nuclear magnetic resonance spectrometer (Bruker Cryomagnet, Oxford) operated under 600 MHz (^1H) and 150 MHz (^{13}C), respectively at room temperature (with high concentration of plasticizers). The chemical shifts (δ ppm) are referenced to the respective solvents and splitting patterns are designed as s (singlet), d (doublet), t (triplet), m (multiplet), br (broad) and bs (broad singlet). The column chromatography was carried out using silica gel (100–200 mesh). The TLC analysis was carried out on double coated silica Merk plates. The ILs were prepared as reported previously by us.^{20,37} The ILs were dried under vacuum for appropriate time and kept in a dry box prior to use.

Preparation of GSO₃H catalyst

The graphene oxide (GO) was synthesized by using a modified Hummer's method.²³ The rGO was synthesized by the chemical reduction of GO using LAH as reported previously.²⁴ The synthesis of GSO₃H was carried out in a standard fume cupboard. Specifically, 1 L nitrogen flushed round-bottomed flask equipped with a condenser and an efficient magnetic stir bar was charged with rGO (5.0 g). Fuming H₂SO₄ (300 mL) was slowly added and the resulting suspension was stirred at room temperature for 1 h. The flask was heated at 120 °C with vigorous stirring for 3 days under nitrogen atmosphere. After completion of the reaction, the reaction mixture was cooled to room temperature and added in portions to a well stirred mixture of crushed ice and water (1 L) in order to quench the reaction.† The resulting black precipitate was filtered and washed repeatedly with water (2 L) followed by acetone (3 × 100 mL). The as-obtained GSO₃H was dried at 60 °C in vacuum overnight for further use.

General procedures for the synthesis of plasticizers

Method A. Citric acid **1**, GSO₃H and an excess of alcohol **2** were placed in a 50 mL round-bottomed flask fitted with a reflux condenser and a magnetic stir bar. The reaction mixture was refluxed at desired temperature for appropriate time. After completion of the reaction, the GSO₃H was filtered off and the solvent **2** was evaporated in a rotary evaporator. The as-obtained product **3** was dried under vacuum and characterized by NMR spectroscopy.

† The reaction should be quenched very carefully as oleum reacts violently with water.

Method B. A 50 mL round-bottomed flask fitted with a reflux condenser and a magnetic stir bar was charged with **1**, GSO₃H and an appropriate solvent. To this stirred mixture, **2** was added in stoichiometric amount *via* a syringe and the reaction mixture was stirred at reflux for appropriate time. After completion of the reaction, the GSO₃H was filtered off and solvent was evaporated in a rotary evaporator. The **3** was occasionally passed through a short silica-gel column and characterized by NMR spectroscopy.

Conclusions

In conclusion, sulfonated graphene (GSO₃H) bearing abundant –SO₃H functional groups have been synthesized in an alternative way at affordable cost. Relative to the traditional mineral and solid acid catalysts, the as-prepared GSO₃H has been proven to be a highly efficient heterogeneous acid catalyst in the synthesis of plasticizer esters, methyl oleate and methyl salicylate. The superior catalytic performance of GSO₃H can be attributed to the synergistic combination of the specific structure, water tolerant character, and the highly acidic–SO₃H functional groups on its surface. These features, in addition, are quite favourable for the stability of catalyst and high mass transfer in the reaction. The experimental results as-described here is expected to contribute to GSO₃H utilization as an alternative yet robust solid acid catalyst for the development of industrially important O- and N-containing heterocycles. Furthermore, the investigations on the efficacy of GSO₃H in biodiesel synthesis and making full use of its by-product, glycerol, is currently underway in our laboratory.

Acknowledgements

This work was supported by National Tsing Hua University (102N1807E1) and the Ministry of Science and Technology (NSC101-2113-M-007-006-MY3) of Taiwan.

Notes and references

- (a) S. L. Rosen, *Fundamental principles of polymeric materials*, ISBN 0-471-57525-9, John Wiley & Sons, New York, NY, USA, 1993; (b) V. Y. Senichev and V. V. Tereshatov, in *Handbook of Plasticizers*, ed. G. Wypych, ChemTec Publishing, New York, NY, USA, 2004, pp. 218–227; (c) Y. Zhu, N. H. Shah, A. W. Malick, M. H. Infeld and J. W. McGinity, *Int. J. Pharm.*, 2002, **241**, 301–310; (d) P. Fedorko, D. Djurado, M. Trznadel, B. Dufour, P. Rannou and J. P. Travers, *Synth. Met.*, 2003, **135–136**, 327–328.
- D. F. Cadogan and C. J. Howick, Plasticizers, in *Ullmann's Encyclopedia of Industrial Chemistry*, Wiley-VCH, Weinheim, 2000, DOI: 10.1002/14356007.a20_439.
- (a) Y. Baoping, CN 101255240 (A), 2008, *Chem. Abstr.*, 2008, **149**, 379449; (b) E. H. Hull and E. P. Frappier, *US Pat.*, 4931 583 (A) 1990.
- (a) L. V. Labrecque, R. A. Kumar, V. Dave, R. A. Gross and S. P. McCarthy, *J. Appl. Polym. Sci.*, 1997, **66**, 1507–1513; (b) V. P. Ghiya, V. Dave, R. A. Gross and S. P. McCarthy, *J.*

- Macromol. Sci., Part A: Pure Appl. Chem.*, 1996, **33**, 627–638; (c) K. Khemani and N. J. McCaffrey, *US Pat.*, 2 008 206 169 (A1), 2008; (d) C. L. Millikin and D. L. Bissett, US 20080206169 A1, 2008.
- 5 Ceresana, Market Study Plasticizers, May 2011, <http://www.ceresana.com/en/market-studies/additives/plasticizers/>.
- 6 (a) R. Maggi, G. Sartori, C. Oro and L. Soldi, *Curr. Org. Chem.*, 2008, **12**, 544–563; (b) M. Noji, Y. Konno and K. Ishii, *J. Org. Chem.*, 2007, **72**, 5161–5167.
- 7 M. Yasunori and A. Masatomo, *Jpn. Pat.*, JP 278840, 2001.
- 8 S. Sheshmani, M. A. Fashapoyeh, M. Mirzaei, B. A. Rad, S. N. Ghortolmesh and M. Yousefi, *Indian J. Chem., Sect. A: Inorg., Bio-inorg., Phys., Theor. Anal. Chem.*, 2011, **50**, 1725–1729.
- 9 Z. Zhifeng, X. Junming, J. Jianchun, L. Yanju and H. Yuanbo, *Bull. Chem. Soc. Ethiop.*, 2011, **25**, 147–150.
- 10 (a) C. Xie, H. Li, L. Li, S. Yu and F. Liu, *J. Hazard. Mater.*, 2008, **151**, 847–850; (b) X. Y. Junming, J. Jianchun, Z. Zhiyue and L. Jing, *Process Saf. Environ. Prot.*, 2010, **88**, 28–30; (c) H. Li, S. Yu, F. Liu, C. Xie and L. Li, *Catal. Commun.*, 2007, **8**, 1759–1762.
- 11 (a) K. S. Novoselov, A. K. Geim, S. V. Morozov, D. Jiang, Y. Zhang, S. V. Dubonos, I. V. Grigorieva and A. A. Firsov, *Science*, 2004, **306**, 666–669; (b) A. K. Geim and K. S. Novoselov, *Nat. Mater.*, 2007, **6**, 183–191.
- 12 (a) C. N. R. Rao, A. K. Sood, K. S. Subrahmanyam and A. Govindaraj, *Angew. Chem., Int. Ed.*, 2009, **48**, 7752–7777; (b) M. J. Allen, V. C. Tung and R. B. Kaner, *Chem. Rev.*, 2009, **110**, 132–145.
- 13 (a) X. Wan, Y. Huang and Y. Chen, *Acc. Chem. Res.*, 2012, **45**, 598–607; (b) Y. Chen, B. Zhang, G. Liu, X. Zhuanga and E.-T. Kang, *Chem. Soc. Rev.*, 2012, **41**, 4688–4707; (c) D. Chen, H. Zhang, Y. Liu and J. Li, *Energy Environ. Sci.*, 2013, **6**, 1362–1387; (d) X. Huang, X. Qi, F. Boey and H. Zhang, *Chem. Soc. Rev.*, 2012, **41**, 666–686; (e) V. Singh, D. Joung, L. Zhai, S. Das, S. I. Khondaker and S. Seal, *Prog. Mater. Sci.*, 2011, **56**, 1178–1271; (f) L. Dai, D. W. Chang, J.-B. Baek and W. Lu, *Small*, 2012, **8**, 1130–1166.
- 14 R. C. Pawar and C. S. Lee, *Appl. Catal., B*, 2014, **144**, 57–65.
- 15 For recent reviews on graphene-based catalysis, see: (a) B. Garg and Y.-C. Ling, *Green Mater.*, 2013, **1**, 47–61 and references there in; (b) B. F. Machado and P. Serp, *Catal. Sci. Technol.*, 2012, **2**, 54–75; (c) C. Su and K. P. Loh, *Acc. Chem. Res.*, 2013, **46**, 2275–2285; (d) D. R. Dreyer, A. D. Todd and C. W. Bielawski, *Chem. Soc. Rev.*, 2014, **43**, 5288–5301; (e) S. Navalon, A. Dhakshinamoorthy, M. Alvaro and H. Garcia, *Chem. Rev.*, 2014, **114**, 6179–6212.
- 16 D. R. Dreyer, H.-P. Jia and C. W. Bielawski, *Angew. Chem., Int. Ed.*, 2010, **49**, 6813–6816.
- 17 For an authoritative detail and conceptual vagueness in graphene-based acid catalysis, see: B. Garg, T. Bisht and Y.-C. Ling, *Molecules*, 2014, **19**, 14582–14614, DOI: 10.3390/molecules190914582.
- 18 (a) J. Ji, G. Zhang, H. Chen, S. Wang, G. Zhang, F. Zhang and X. Fan, *Chem. Sci.*, 2011, **2**, 484–487; (b) H. Zhang, W. P. Low and H. K. Lee, *J. Chromatogr. A*, 2012, **1233**, 16–21; (c) J. Lu, W. Liu, H. Ling, J. Kong, G. Ding, D. Zhou and X. Lu, *RSC Adv.*, 2012, **2**, 10537–10543; (d) B.-Y. Hua, J. Wang, K. Wang, X. Li, X.-J. Zhu and X.-H. Xia, *Chem. Commun.*, 2012, **48**, 2316–2318; (e) M. Jana, P. Khanra, N. C. Murmu, P. Samanta, J. H. Lee and T. Kuila, *Phys. Chem. Chem. Phys.*, 2014, **16**, 7618–7626; (f) Z. Xiong, T. Gu and X. Wang, *Langmuir*, 2014, **30**, 522–532; (g) G. Zhao, L. Jiang, Y. He, J. Li, H. Dong, X. Wang and W. Hu, *Adv. Mater.*, 2011, **23**, 3959–3963.
- 19 F. Liu, J. Sun, L. Zhu, X. Meng, C. Qi and F.-S. Xiao, *J. Mater. Chem.*, 2012, **22**, 5495–5502.
- 20 B. Garg and Y.-C. Ling, *Tetrahedron Lett.*, 2012, **53**, 5674–5677.
- 21 (a) J.-Y. Liu, B. Garg and Y.-C. Ling, *Green Chem.*, 2011, **13**, 2029–2031; (b) B. Garg and Y.-C. Ling, *J. Chin. Chem. Soc.*, 2014, **61**, 737–742.
- 22 B. C. Brodie, *Philos. Trans. R. Soc. London*, 1859, **149**, 249–259.
- 23 F. Kim, J. Luo, R. Cruz-Silva, L. J. Cote, K. Sohn and J. Huang, *Adv. Funct. Mater.*, 2010, **20**, 2867–2873.
- 24 A. Ambrosi, C. K. Chua, A. Bonanni and M. Pumera, *Chem. Mater.*, 2012, **24**, 2292–2298.
- 25 Y. Si and E. T. Samulski, *Nano Lett.*, 2008, **8**, 1679–1682.
- 26 A. C. Ferrari and J. Robertson, *Phys. Rev. B: Condens. Matter Mater. Phys.*, 2000, **61**, 14095–14107.
- 27 X. Fan, W. Peng, Y. Li, X. Li, S. Wang, G. Zhang and F. Zhang, *Adv. Mater.*, 2008, **20**, 4490–4493.
- 28 L. Wang, J. Zhang, S. Yang, Q. Sun, L. Zhu, Q. Wu, H. Zhang, X. Meng and F.-S. Xiao, *J. Mater. Chem. A*, 2013, **1**, 9422–9426.
- 29 K. S. Novoselov, A. K. Geim, S. V. Morozov, D. Jiang, M. I. Katsnelson, I. V. Grigorieva, S. V. Dubonos and A. A. Firsov, *Nature*, 2005, **438**, 197–200.
- 30 J. P. Osegovic and R. S. Drago, *J. Phys. Chem. B*, 2000, **104**, 147–154.
- 31 M. M. Antunes, P. A. Russo, P. V. Wiper, J. M. Veiga, M. Pillinger, L. Mafra, D. V. Evtuguin, N. Pinna and A. A. Valente, *ChemSusChem*, 2014, **7**, 804–812.
- 32 D. Margolese, J. A. Melero, S. C. Christiansen, B. F. Chmelka and G. D. Stucky, *Chem. Mater.*, 2000, **12**, 2448–2459.
- 33 (a) A. Dhakshinamoorthy, M. Alvaro, P. Concepción, V. Fornés and H. Garcia, *Chem. Commun.*, 2012, **48**, 5443–5445; (b) A. Dimiev, L. B. Alemany and J. M. Tour, *ACS Nano*, 2013, **7**, 576–588; (c) S. Eigler, C. Dotzer, F. Hof, W. Bauer and A. Hirsch, *Chem.-Eur. J.*, 2013, **19**, 9490–9496.
- 34 R. Pal, T. Sarkar and S. Khasnobis, *ARKIVOC*, 2012, (i), 570–609.
- 35 S. Suganuma, K. Nakajima, M. Kitano, D. Yamaguchi, H. Kato, S. Hayashi and M. Hara, *J. Am. Chem. Soc.*, 2008, **130**, 12787–12793.
- 36 V. I. Paârvulescu and C. Hardacre, *Chem. Rev.*, 2007, **107**, 2615–2665.
- 37 B. Garg, S.-L. Lei, S.-C. Liu, T. Bisht, J.-Y. Liu and Y.-C. Ling, *Anal. Chim. Acta*, 2012, **757**, 48–55.
- 38 M. Hara, *Energy Environ. Sci.*, 2010, **3**, 601–607.
- 39 M. Rahman and C. S. Brazel, *Prog. Polym. Sci.*, 2004, **29**, 1223–1248.
- 40 M. Hara, *Energy Environ. Sci.*, 2010, **3**, 601–607.